

# Delve into Visual Contrastive Decoding for Hallucination Mitigation of Large Vision-Language Models

Yi-Lun Lee<sup>†</sup> Yi-Hsuan Tsai<sup>‡</sup> Wei-Chen Chiu<sup>†</sup>

<sup>†</sup>National Yang Ming Chiao Tung University <sup>‡</sup>Atmanity

{yllee10727, walon}@cs.nctu.edu.tw, yhtsai@atmanity.io

## Abstract

While large vision-language models (LVLMs) have shown impressive capabilities in generating plausible responses correlated with input visual contents, they still suffer from hallucinations, where the generated text inaccurately reflects visual contents. To address this, recent approaches apply contrastive decoding to calibrate the model’s response via contrasting output distributions with original and visually distorted samples, demonstrating promising hallucination mitigation in a training-free manner. However, the potential of changing information in visual inputs is not well-explored, so a deeper investigation into the behaviors of visual contrastive decoding is of great interest. In this paper, we first explore various methods for contrastive decoding to change visual contents, including image down-sampling and editing. Downsampling images reduces the detailed textual information while editing yields new contents in images, providing new aspects as visual contrastive samples. To further study benefits by using different contrastive samples, we analyze probability-level metrics, including entropy and distribution distance. Interestingly, the effect of these samples in mitigating hallucinations varies a lot across LVLMs and benchmarks. Based on our analysis, we propose a simple yet effective method to combine contrastive samples, offering a practical solution for applying contrastive decoding across various scenarios. Extensive experiments are conducted to validate the proposed fusion method among different benchmarks. Code is available at [https://github.com/YiLunLee/VCD\\_Analysis](https://github.com/YiLunLee/VCD_Analysis).

## 1. Introduction

Recent large vision-language models (LVLMs) [2, 5, 18] have shown strong capabilities of yielding detailed and plausible responses correlated to the visual inputs. However, stemming from LLMs, LVLMs also suffer from “hallucination”, where the generated responses are fluent and semantically coherent but may conflict with input visual contents, leading to a risk of producing fabri-

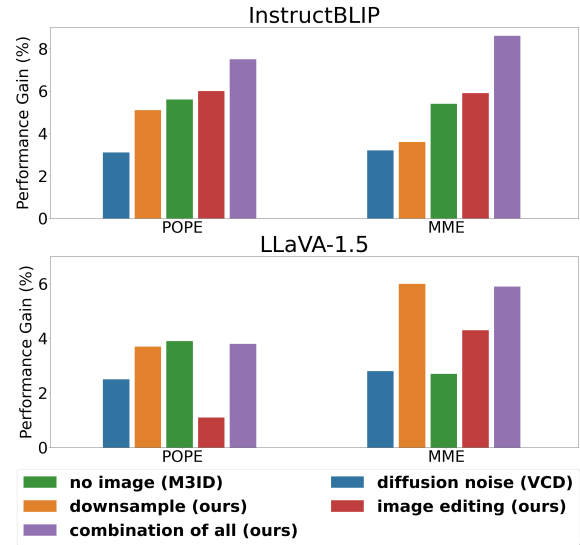


Figure 1. Performance gain brought by visually changed samples across different LVLMs and benchmarks (POPE [15] and MME [8]). We find that contrastive decoding with different samples reaches varying performance gains across benchmarks and LVLMs, motivating us to develop a solution to leverage the advantage of each CD method in a combined manner.

ated information. To mitigate hallucinations in LVLMs, various approaches have been explored, including learning from human feedback or preference [19, 22, 28], fine-tuning LVLMs with newly proposed hallucination-calibration datasets [10, 17], training a post-hoc calibrator to rectify hallucinated responses [25, 30], and designing novel decoding strategies [7, 13, 24]. However, most of them require collecting new datasets and fine-tuning LVLMs, which can be a huge burden with manual efforts and computational resources, as well as less flexible to deploy in specific domains.

In contrast, training-free decoding strategies such as contrastive decoding (CD) [4, 7, 13, 14, 24], which adjusts predicted logits via subtracting the logits from contrastive samples (e.g., distorted visual inputs), serves as a simple yet ef-

fective approach to mitigate hallucinations in LVLMs without additional datasets and fine-tuning. The insight is that the visual input with distortion exacerbates hallucinations happening in the response, and thus, CD subtracts the hallucinated contents from the original distribution to mitigate hallucinations. For example, VCD [13] adds Gaussian noise to the input image in a diffusion manner, which increases the uncertainty of LVLMs’ responses and thus strengthens the probability of producing hallucinations as contrastive samples. M3ID [7] directly removes the visual input, forcing the LVLMs to contrast with the bias from pre-trained LLMs. ICD [24] introduces deceptive instruction for the visual-text interface (e.g., Q-Former [5]), exacerbating the misalignment between visual and text embedding.

Inspired by the success of contrastive decoding with visually changed samples, we further explore the other two ways of distorting visual inputs to serve as contrastive samples, including image downsampling and editing. The former reduces high-frequency details from images, while the latter inserts specific hallucination contents into the input image. We hypothesize that different visually changed samples bring various outcomes of mitigating hallucinations. To verify this, we provide the performance gain of different CD methods on various benchmarks and LVLMs in Figure 1. We find that the efficacy of different CDs varies across LVLMs and tasks. For example, contrastive decoding with image editing improves the InstructBLIP [5] on the POPE [15] and MME [8] benchmarks the most but has a minor improvement for LLaVA-1.5 [18] on the POPE benchmark. The observation indicates that different samples exhibit significantly varied suitability across settings, which is practically challenging to determine which contrastive samples to use when applying to novel datasets and tasks. This encourages us to delve into the impact of using various CDs and thus develop a simple solution to leverage the advantage of each CD method.

To investigate the effect of each visually changed sample, we conduct thorough analysis from the perspective of the probability distribution of generated words, including entropy and predicted distribution distance. We further delve into models’ behavior of various CD methods on different benchmarks with different pre-trained LVLMs. Interestingly, we observe that different CDs exhibit significantly varied suitability across LVLMs and datasets. In general, visually changed samples with higher entropy of next-token prediction act as more effective contrastive samples for mitigating hallucination.

Based on these findings, it can be a practical challenge to determine the suitable type of CDs to mitigate hallucinations when deploying the LVLMs in a new dataset or downstream task. To this end, we propose a simple yet effective fusion method to apply all different types of CDs according to their predictions’ behavior. Specifically, we leverage

entropy as guidance to automatically determine the scale of influence of contrastive decoding. Extensive experiments on different benchmarks verify the efficacy of the proposed fusion method in different situations, demonstrating that applying various visually changed samples with an entropy-weighted combination serves as a general solution to mitigate hallucinations in real-world scenarios across datasets and LVLMs. Our main contributions are as follows:

- We explore various visual CDs to produce visually changed samples, such as image downsampling and editing, and investigate the impact of these samples for mitigating hallucinations in LVLMs.
- We conduct a thorough analysis of various CDs using probability-level metrics on LVLM’s response, demonstrating that each contrastive sample has its distinct benefit across tasks and datasets.
- Based on our analysis, we further propose a simple yet effective fusion method to leverage different contrastive samples, serving as a more practical and general solution to mitigate hallucinations with various LVLMs on different tasks and datasets.

## 2. Related Work

### 2.1. Hallucination Mitigation in LVLMs

With advancements in LLMs, various LVLMs incorporate visual encoders like CLIP [20] with LLMs (e.g., LLaMA [23], Vincuna [29], or Qwen [1]) to yield reasonable and detailed responses related to visual contents, including but not limited to InstructBLIP [5], LLaVA-1.5 [18], Qwen-VL [2], MiniGPT-4 [31], and MPLG-Owl2 [26]. Despite the promising performance, these LVLMs still suffer from hallucinations, where the generated responses are inaccurately grounded with image contents. To address this, several approaches are proposed from different aspects: **learning with human feedback and preference** methods [19, 22, 28] either conduct reinforcement learning with the human feedback [22] or leverage Direct Preference Optimization (DPO) framework [21] to fine-tune LVLMs with DPO datasets generated by GPT-4v [28] or CLIP Ranking [19]; **finetuning** methods [10, 17] first introduce newly collected hallucination-calibration datasets (e.g., LRV-Instruct [17] and M-HalDetect [10]) and fine-tune LVLMs with them to prevent hallucinations; **post-hoc** methods [27, 30] includes post-processing calibration with external models [27] or training post-hoc revisors to correct hallucinated responses [30].

However, most of the above-mentioned approaches have practical drawbacks: they require significant manual effort to create hallucination-specific datasets and involve fine-tuning LVLMs or training post-hoc revisors. In contrast, some studies focus on **adjusting decoding strategies**, offering a more practical solution without additional train-

ing or data. OPERA [12] investigates the over-trust issue in LVLMs and penalizes tokens prone to hallucinations. CGD [6] leverages CLIP [20] to select candidate sentences grounded with image contents. As a mainstream of the decoding process, contrastive decoding (CD) [4, 7, 13, 14, 24, 32] mitigates hallucinations by adjusting logits based on contrastive samples. In this paper, we mainly focus on exploring contrastive decoding approaches.

## 2.2. Contrastive Decoding

Contrastive decoding [14] is oriented from mitigating the hallucination of LLMs, leveraging the contrast between expert and amateur models to amplify good expert behavior and diminish undesired amateur behavior. To extend contrastive decoding for LVLMs, several approaches [4, 7, 13, 24, 32] are proposed with different designs of contrastive samples prone to producing hallucinations. As a pioneer, VCD [13] increases the uncertainty of visual inputs by adding Gaussian noise in a diffusion manner, producing more hallucinated contents. M3ID [7] directly contrasts the predictions from the original visual inputs with those of pre-trained LLMs without input images, which induce hallucinations from language priors. IBD [32] finetunes LVLM to be image-biased LVLM via amplification of attention on visual tokens and then contrast with conventional LVLM, which is likely text-biased to mitigate the hallucination. ICD [24] adjusts the instruction for the Q-Former [5] with deceptive prompts to destroy the alignment between visual and text embeddings, leading to more likelihoods of producing hallucinations. HALC [4] selects different field of views (FOVs) based on decoding probabilities and performs contrastive decoding of FOV pairs to find the optimal outputs matching the visual input.

Despite the impressive performance, the potential of using visually changed samples in LVLMs remains underexplored. To this end, we first explore different manipulations of image contents for creating visually changed samples and investigate the prediction-level metrics on LVLMs’ response and revision behaviors of contrastive decoding. Moreover, based on these observations, we propose an effective fusion method to leverage the strengths of different visually changed samples.

## 3. Visual Contrastive Decoding

### 3.1. Preliminaries

**Decoding process of LVLMs.** We first introduce the generation paradigm of LVLMs, involving an LVLM parameterized by  $\theta$ , visual input  $v$ , and textual query  $x$ . Then LVLM considers the contextual information from the visual input  $v$  to yield relevant responses  $y$  to the textual query  $x$ , where the responses are generated auto-regressively via sampling from the distribution conditioned on visual input  $v$

and textual query  $x$ . The auto-regressive generation process can be formulated as follows:

$$y_t \sim p_\theta(y_t|v, x, y_{<t}) = \text{softmax}(\text{logit}_\theta(y_t|v, x, y_{<t})). \quad (1)$$

Here,  $y_t$  denotes the token at time step  $t$ , and  $y_{<t}$  represents the sequence of generated tokens up to the time step  $(t - 1)$ . However, during the decoding process, the hallucination response may occur in several situations: 1) the visual contextual information is captured unsuccessfully, 2) LLM priors suppress the information from image embeddings, and 3) statistics from pre-trained datasets affect the responses with the similar scene learned previously.

### Contrastive decoding with visually changed samples.

To mitigate hallucinations, several approaches [7, 13, 14, 24] are proposed to adjust the decoding process in a contrastive manner. Specifically, samples that are changed with less visual information are introduced to produce a hallucination response due to insufficient visual contents. Then, these hallucinated contents are subtracted from the original response during the contrastive decoding process to prevent LVLMs from producing hallucinations. That is, the original logits of the next token are subtracted by those of contrastive samples, where the formula can be denoted as:

$$p_{cd}(y_t|v, v_{cd}, x, y_{<t}) = \text{softmax}[(1 + \alpha)\text{logit}_\theta(y_t|v, x, y_{<t}) - \alpha(\text{logit}_\theta(y_t|v_{cd}, x, y_{<t}))], \quad (2)$$

where  $v_{cd}$  is the visually changed sample and  $\alpha$  is the weight to control the effect of differences between the two distributions.

### 3.2. Visually Changed Samples in Different Aspects

The high-level concept behind contrastive decoding is to create visually changed (or distorted) samples serving as contrastive samples, which are more likely to produce hallucinated contents due to the reduced image information. Previous works [7, 13] have explored two ways, adding diffusion noise to the image or simply removing the image. Inspired by these methods, we further explore two distinct types: image downsampling and editing. The illustration of visually changed samples is shown in Figure 2.

**Diffusion noise.** As a pioneer in applying contrastive decoding to multimodal scenarios, VCD [13] proposes applying a diffusion process following [11] to add Gaussian noise  $\mathbf{N}$  onto the original input image  $v_o$ . During the diffusion process, the diffusion function  $q$  incrementally adds a small amount of Gaussian noise for  $N$  steps, producing distorted image sequences  $\{v_1, v_2, \dots, v_N\}$ . The diffusion process can be formed:

$$q(v_n|v_{n-1}) = \mathbf{N}(v_n; \sqrt{1 - \gamma v_{n-1}}, \gamma \mathbf{I}),$$

$$q(v_N|v_o) = \prod_{n=1}^N q(v_n|v_{n-1}), \quad (3)$$

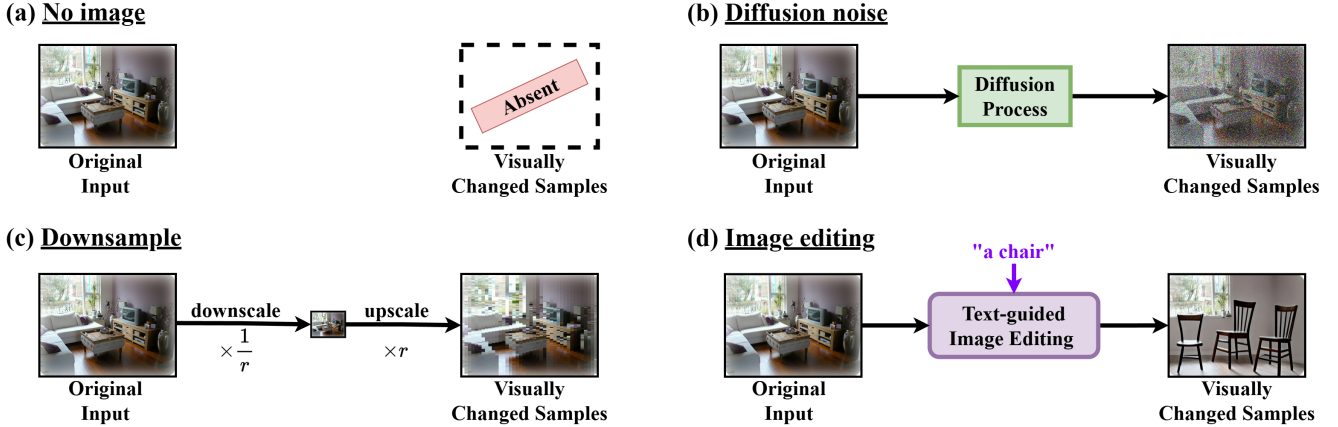


Figure 2. Illustration of various visually changed samples for different contrastive decoding strategies.

where  $N$  is the total steps of adding noise and  $\gamma$  controls the amount of noise added in each step. As the noise step  $n$  increases, the original image  $v_o$  gradually loses the visual contextual information, thus increasing the uncertainty of the next token prediction and amplifying the probability of hallucination. After  $N$  diffusion steps, we obtain the visually changed samples with diffusion noise  $v_{cd} = v_N$ .

**No image.** As mentioned before, one of the reasons for producing hallucinations is the dominant LLM priors learned from the pre-training phase. To mitigate such hallucinations, M3ID [7] contrasts the responses of LVLMs with those of LLMs, where the input image is absent. Since no visual information is provided, the LLMs follow the learned priors to generate a related response to the textual query. The contrastive decoding process is as follows:

$$p_{cd}(y_t|v, v_{cd}, x, y_{<t}) = \text{softmax}[(1 + \alpha)(\text{logit}_{\theta}(y_t|v, x, y_{<t}) - \alpha(\text{logit}_{\theta_{LLM}}(y_t|x, y_{<t}))], \quad (4)$$

where  $\theta_{LLM}$  denotes parameters of the pre-trained LLM.

**Image downsampling.** In addition to the above two methods, we propose downsampling images to a lower resolution, where high-frequency details are reduced, to serve as another type of visually changed sample. Given an image size, we first downscale each side of the image by ratio  $\frac{1}{r}$  and then directly upscale the output by ratio  $r$  to meet the original size. The downsampling process can be denoted as:

$$v_{cd} = \text{resize}(\text{resize}(v, \frac{1}{r}), r), \quad (5)$$

where  $\text{resize}()$  is the function to resize the image by the given ratio. In our experiments, we set  $r = 32$  by default.

**Image editing.** Contrasting with the existing methods, image editing provides another aspect of creating visually

changed samples. Recently, text-driven image editing models [3, 9, 16] present impressive ability to edit specific contents grounded with the given text instruction or captions without losing the similarity to the original image. We apply one of the text-driven image editing models, Instruct-pix2pix [3], to edit the original visual input  $v$  given the editing textual instructions  $t_{edit}$ , and regard the resultant edited image as a visually changed sample for contrastive decoding. The editing process can be denoted as:

$$v_{cd} = \text{edit}(v, t_{edit}). \quad (6)$$

The instructions can be obtained in different ways based on the downstream tasks. The instruction for question-answering tasks (which we mainly focus on) is the queried objects or contents from the questions. We provide more examples of instructions and their corresponding edited images in the supplementary material.

## 4. Analysis on Visual Contrastive Encoding

Although prior studies (e.g., VCD [13] and M3ID [7]) have demonstrated impressive improvement on LVLMs via contrastive decoding with visually changed samples (e.g., adding noise and removing the image, respectively), The effectiveness of using different visual CD methods to mitigate the hallucination issue is not well explored yet. As mentioned in Sec. 1, we observe that on different benchmarks (POPE [15] and MME [8]), the performance gain brought from different visually changed samples varies across LVLMs and tasks.

We hypothesize that applying different visually changed samples yields varying influences on mitigating hallucinations. Thus, we conduct several analysis on the prediction-level statistics to understand behaviors of using each visually changed sample, including entropy/confidence, probability distribution distance, revised outcomes' behaviors,

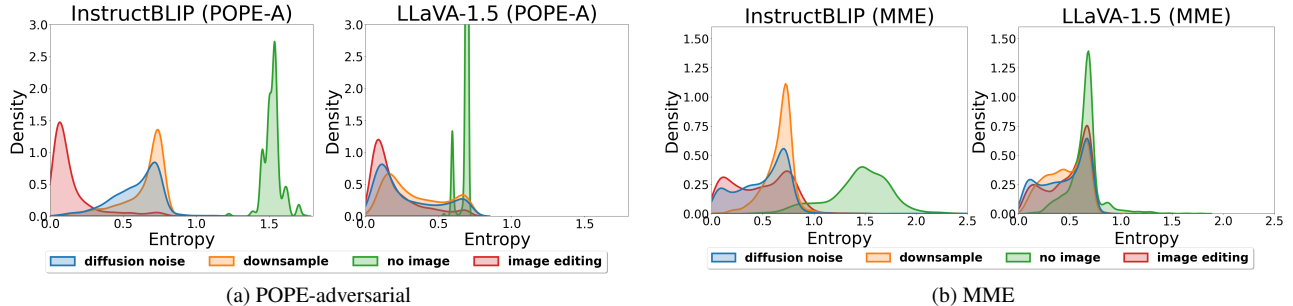


Figure 3. The entropy analysis on the POPE and MME benchmarks.

and the pair-wise relationship of rectified answers. To better investigate this without randomness, we focus on the first token of the response using the Yes-No Question task (i.e., POPE and MME), where the next token is selected with the highest probability.

#### 4.1. Benchmarks and LVLMS

**Benchmarks.** POPE [15], the Polling-based Object Probing Evaluation, aims to assess the object hallucination. This benchmark consists of Yes-No question-answering pairs related to the corresponding image, querying the LVLMS to answer whether a specific object exists in the image or not. The ratio of Yes and No questions is balanced (i.e., 50% vs 50%). Within this benchmark, there are three different difficulties of queried non-existent objects, including *random*, *popular*, and *adversarial*. In the *random* setting, the non-existent objects are selected from all the objects in datasets randomly, while the *popular* setting selects non-existent objects from the high-frequency pool. For the *adversarial* setting, the non-existent objects are selected from the co-occurrence objects related to the queried image scene.

MME [8], a more challenging benchmark for assessing hallucination from multiple perspectives. It contains 14 Yes-No question-answering tasks, including four coarse-grained perception tasks, six fine-grained perception tasks, and four cognition-focus tasks.

**LVLMS backbones.** We follow prior works [13] to evaluate the prediction tendency and behaviors of different visually changed samples using InstructBLIP [5], LLaVA-1.5 [18], and Qwen-VL [2]. Specifically, these LVLMS are comprised of three components: image encoder, visual-textual interface, and language decoder. The main difference among these three LVLMS is the design of the visual-textual interface: InstructBLIP uses the Q-Former (a transformer) to extract task-relevant image features related to the textual query; LLaVA-1.5 directly projects visual embedding into language embedding with multi-layer perception (MLP), and Qwen-VL utilizes a position-aware vision-language adapter (a cross-attention layer) to compress image features. These differences in the visual-textual inter-

face may result in different output behaviors of visually changed samples. To better illustrate the observation within the page limit, we discuss InstructBLIP and LLaVA-1.5 in the manuscript, leaving comparisons with all LVLMS in the supplementary materials.

#### 4.2. Analysis with Entropy

We investigate the behavior of each visually changed sample in terms of entropy (i.e., confidence). It is acknowledged that entropy represents the uncertainty of the prediction. Previous work [13] demonstrates that visual uncertainty amplifies the language priors and statistical bias, which leads to hallucinations. The entropy can serve as an indicator to determine the extent of inducing hallucinations given different visually changed samples. To delve into more concrete observations using entropy, we visualize the entropy distribution of the first token in the Yes-No question, as shown in Figure 7. Visually changed samples have distinct properties of entropy across different LVLMS and benchmarks, which reflects the design of manipulation on visual inputs. We draw several observations:

1) **No image** method only contrasts with the response from the pre-trained LLM without image information, producing more noisy and unpredictable outputs.

2) **Downsample** and **diffusion noise** methods have similar entropy distributions, indicating a similar effect of losing some image information to increase the uncertainty of output predictions.

3) Different from other visually changed samples, the **image editing** method provides a more specific modification related to the textual instruction extracted from the textual query of LVLMS, where the editing goal is to insert the queried objects into the image. Hence, the entropy is very low in comparison with others on POPE, which only focuses on object existence. In contrast, the MME benchmark contains various perception and cognition tasks; the editing difficulty of the queried fine-grained contents increases, and thus, edited images may fail to be consistent with the original images.

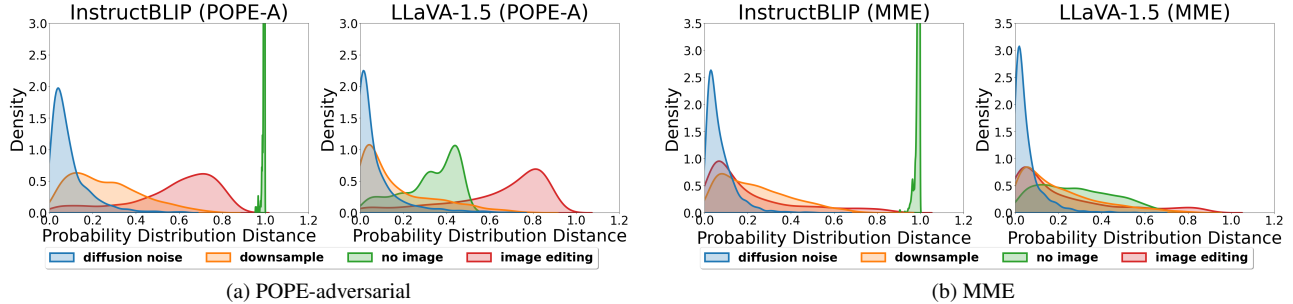


Figure 4. The analysis of probability distribution distance on the POPE and MME benchmarks.

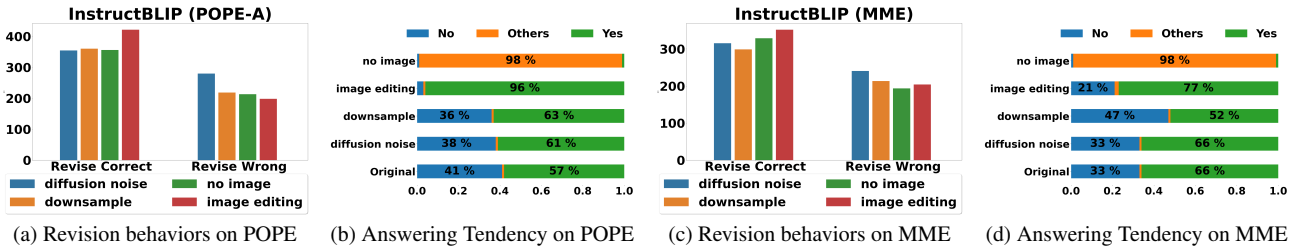


Figure 5. The revision behaviors and answering tendency of InstructBLIP with different visually changed samples.

### 4.3. Analysis with Probability Distribution Distance

In addition to the entropy, we further measure the probability distribution distance (PDD) between the original and CD predictions, which is also investigated in [7]. Here, we mainly use the Hellinger distance to estimate the distance between probability distributions, defined as  $H(p, q) = 2^{1/2} \sqrt{\sum_{i=1}^k (\sqrt{p_i} - \sqrt{q_i})^2}$ , where  $p = (p_i)_{i \in |k|}$  and  $q = (q_i)_{i \in |k|}$  are discrete probability distributions. Intuitively, when the distance increases, the prediction distribution of the original visual input and visually changed sample differs more, leading to a high risk of obtaining hallucination results from visually changed samples. According to the results shown in Figure 9, we draw several observations:

1) **No image** method presents distinct distributions of PDD with InstructBLLIP and LLaVA-1.5. This phenomenon indicates that the language priors learned from LVLMs are different.

2) **Diffusion noise** method has PDD distribution centralized at lower PDD values, demonstrating that even the uncertainty of visual inputs is enhanced with added noises, the prediction distribution is still similar to the original input. **Downsample** method also has lower PDD values, where the overall distribution is smoother, meaning that parts of downsampled samples change their predictions due to the lost of high-frequency details.

3) Different from others, **image editing** method obtains the PDD distribution with higher values on POPE but lower values on MME. As mentioned previously, editing a

specific object on images is easier than editing fine-grained contents. Therefore, edited images with non-existent objects results in a positive response in LVLMs for answering the corresponding question that queries non-existent objects. On the contrary, editing methods may fail to edit the image with fine-grained contents, leading to similar visual contents, thus having a closer prediction distribution to the original one.

### 4.4. Revision Behaviors

To investigate the behavior of each contrastive sample, we focus on three metrics: revise-correct samples, revise-wrong samples, and the predicting tendency on the POPE and MME benchmarks. Revise-correct samples indicate that the contrastive decoding revises the original response with the correct answers, while revise-wrong samples present the opposite case. Predicting tendency is the tendency of LVLMs to answer Yes-No Questions with or without contrastive decoding, including yes, no, and others. The results are shown in Figure 5. We draw several observations:

1) As shown in Figure 5 (a) and (c), the results present that the contrastive decoding with different visually changed samples adjusts both correct and incorrect answers, where the revise-correct samples are more than revise-wrong ones. This phenomenon reveals that: although these CD methods appear to improve the overall performance, it is because that the number of revise-correct samples outweighs the number of revise-wrong samples.

However, in practical applications, the revise-wrong case also emerges as a risk for misleading users.

2) **downsample** and **diffusion noise** methods have more revise-wrong samples than the other two methods, which is consistent with the observation on PDD. The visually changed samples with lower PDD values present similar output prediction as the original input, leading to a high risk of subtracting the probability of correct answers. In contrast, the **image editing** method has PDD distribution with large values, indicating the dissimilar output prediction to the original prediction. Therefore, when the original prediction is correct, contrastive decoding with image editing samples may not affect the output distribution, resulting in fewer revise-wrong samples.

3) We show the answering tendency of each visually changed sample in Figure 5 (b) and (d). We find that samples with loss of information (i.e., downsample and diffusion noise methods) tend to predict yes answers more, while samples with dramatic changes like no image or inserting queried specific objects/contents have nearly unified answers, e.g., almost “yes” for image editing and “others” for no image. Such varying prediction tendencies suggest that the output prediction affected by these CD methods are different, and there are likely existing complementary properties among these visually changed samples.

#### 4.5. Pairwise Overlap of Rectified Answers

Based on the above observation of revision behaviors, we investigate the complementary properties among different CD methods. Specifically, we calculate the pairwise overlap of rectified answers among different visually changed samples. That is, the Jaccard similarity coefficient (known as IoU) is computed in the revise-correct set using any of the two CD methods. As shown in Figure 12, a lower score means a higher complement between two CD methods. Interestingly, results show that most pairwise scores are low, demonstrating the distinct effect of each CD method to rectify answers. This evidence motivates us to design a combined approach that leverages the strengths of each contrastive sample.

### 5. Fusion of Visual Contrastive Decoding

According to the observations studied above, we find that one visually changed sample may exhibit better performance under some settings due to its distinct behaviors and output distributions. Instead of manually selecting the best contrastive decoding method when encountering new tasks or datasets, we propose to apply all the visually changed samples and fuse their influence, which can be a more general approach to mitigate hallucinations in practice.

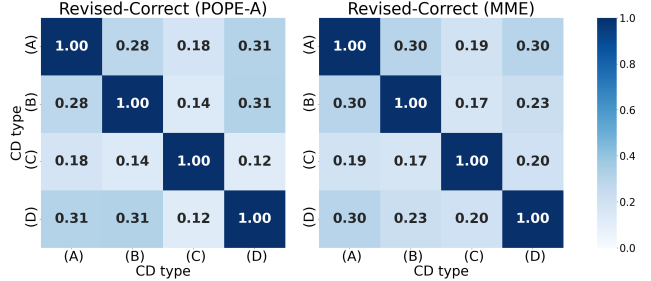


Figure 6. The pairwise overlap of revise-correct samples. CD types consist of (A) diffusion noise, (B) downsample, (C) no image, and (D) image editing.

#### 5.1. Naive Fusion

An intuitive approach to fuse the effect of different visually changed samples is to combine them with the same weight. According to (2), the decoding with fusion of several visually changed samples can be derived as:

$$p_{cd}(y_t|v, v_{cd}, x, y_{<t}) = \text{softmax}[(1 + \alpha)\text{logit}_\theta(y_t|v, x, y_{<t}) - \alpha \sum_{i=1}^k \text{logit}_\theta(y_t|v_{cd_i}, x, y_{<t})], \quad (7)$$

where the  $\{v_{cd_1}, v_{cd_2}, \dots, v_{cd_k}\}$  is the set of different visually changed samples.

#### 5.2. Entropy-weighted Fusion

As studied above, when the entropy is higher, the LVM is less confident in its response. Visually changed samples with a higher entropy can be more likely to yield the hallucinated response, which is more suitable for serving as a contrastive sample. Therefore, we fuse the different types of visually changed samples with the corresponding entropy of outputs as the weight. We then reformulate (2) as:

$$p_{cd}(y_t|v, v_{cd}, x, y_{<t}) = \text{softmax}[\text{logit}_\theta(y_t|v, x, y_{<t}) - \sum_{i=1}^k e_i(\text{logit}_\theta(y_t|v, x, y_{<t}) - \text{logit}_\theta(y_t|v_{cd_i}, x, y_{<t}))], \quad (8)$$

where  $e_i$  is the entropy of output distribution for a visually changed sample  $v_{cd_i}$ . Note that, a similar formulation can be also derived for the case of using probability distribution distance, in which we will include details in the supplementary material.

#### 5.3. Quantitative Results

We compare our fusion methods with other contrastive decoding methods with the single visually changed sample in Table 1. We demonstrate the accuracy under several settings with different LVMs (i.e., InstructBLIP [5], LLaVA-1.5 [18], and Qwen-VL [2]) and benchmarks (POPE [15]

Table 1. The results on the Yes-No question tasks, including POPE and MME. Please refer to Sec. 5.1 and 5.2 for the formulation of fusion methods. P-R denotes the *random* task of POPE, P-P denotes the *popular* task of POPE, and P-A denotes the *adversarial* task of POPE. The best performance within each set is marked **bold**, and the second highest performance is underlined.

VQA (Y/N)	InstructBLIP				LLaVA-1.5				QwenVL				Overall
Benchmark (Acc)	P-R	P-P	P-A	MME	P-R	P-P	P-A	MME	P-R	P-P	P-A	MME	All
Original	0.825	0.733	0.752	0.688	0.832	0.817	0.788	0.705	0.847	0.851	0.822	0.720	0.785
diffusion noise (VCD [13])	0.858	0.805	0.779	0.720	0.863	0.842	0.805	0.733	0.865	0.865	0.832	0.747	0.810
no image (M3ID [7])	<u>0.880</u>	0.835	0.802	0.742	0.871	<b>0.856</b>	<b>0.827</b>	0.732	0.868	<u>0.871</u>	0.837	0.733	0.821
downsample	0.878	0.824	0.801	0.724	<b>0.879</b>	<b>0.856</b>	0.811	<u>0.765</u>	<b>0.875</b>	<u>0.871</u>	<u>0.842</u>	<u>0.764</u>	0.824
image editing	0.860	0.839	0.829	0.747	0.832	0.826	0.811	0.748	0.845	0.838	0.824	0.763	0.814
naive fusion	0.864	0.840	<b>0.832</b>	<b>0.774</b>	0.862	0.847	<b>0.827</b>	<b>0.779</b>	0.865	0.860	0.839	<b>0.768</b>	<u>0.830</u>
entropy-weighted fusion	<b>0.890</b>	<b>0.857</b>	0.828	<b>0.774</b>	0.872	<b>0.856</b>	0.824	0.764	<u>0.872</u>	<b>0.873</b>	<b>0.844</b>	0.749	<b>0.833</b>
PDD-weighted fusion	0.876	<u>0.849</u>	<u>0.830</u>	<u>0.760</u>	<u>0.872</u>	<u>0.849</u>	<u>0.825</u>	0.755	0.866	0.861	0.838	0.762	0.829

Table 2. The results of overall performance on the Yes-No question tasks, including POPE and MME. The results below are entropy-weighted fusion methods with different combinations of visually changed samples. The best performance within each set is marked **bold**, and the second highest performance is underlined.

VQA (Y/N)	Overall
Benchmark (Acc)	All
Original	0.785
diffusion noise (VCD [13]) (A)	0.810
no image (M3ID [7]) (B)	0.821
downsample (C)	0.824
image editing (D)	0.814
A+B	0.826
A+B+C	<u>0.829</u>
A+B+C+D	<b>0.833</b>

and MME [8]), where we highlight the averaged number over all settings in the last column as the overall accuracy. In every single setting (i.e., each column indicates a specific task and LVL), applying fusion of all visually changed samples (i.e., methods in the bottom of the table) has the best or second-best performance compared to other single-sample methods, validating our motivations to combine different samples with complementary properties to mitigate hallucinations. In addition, we find that our down-sample method reaches the best overall performance among all single-sample methods, showcasing a more effective CD strategy than other existing methods.

Moreover, we compare different fusion methods, including naive fusion, entropy-weighted fusion, and PDD-weighted fusion, where the naive fusion directly combines all the visually changed samples while the latter two fusions are weighted according to the entropy and probability distribution distance of outputs. As described in Sec. 4.2 and 4.3, one of the main differences between these two metrics is the distribution of the image-editing method on POPE, which has lower values of entropy but higher values of PDD. Considering the performance in Table 1 and the above observations, we find that entropy-weighted fusion can alleviate

the negative influence of image editing on the POPE benchmark via a smaller value of entropy and keep its strength on the MME benchmark with a higher value of entropy. This evidence validates our expectation that entropy represents the uncertainty of outputs correlating with the likelihood of producing hallucinations, which is more suitable as the fusion weights on different visually changed samples.

#### 5.4. Combinations of Fusion Methods

We have shown that entropy-weighted fusion with all visually changed samples is more robust to hallucinations than solely applying a specific visually changed sample; however, one question may emerge: “Do we need to fuse all designed visually changed samples?”. To further study this, we conduct an ablation study of different combinations of fusion methods in Table 2, where the combination ranges from fusing two to four visually changed samples. We find that fusion with more visually changed samples yields better overall performance, demonstrating that it is more general method than selecting specific combinations to be deployed for practical applications on novel data and tasks. More results are provided in the supplementary materials.

## 6. Conclusions

In this paper, we delve into visual contrastive decoding with various visually changed samples to mitigate hallucinations for large vision-language models. We first explore new visually changed samples from different aspects, including downsampling and image editing. We conduct thorough prediction-level analysis to investigate the prediction behaviors of visually changed samples, concluding that different visually changed images exhibit significantly varied suitability across different LVLs and datasets. To this end, we propose an entropy-weighted fusion method to leverage the complementary property from visually changed samples based on the entropy of predictions, which is proportional to the likelihood of hallucinations. Experimental results showcase the efficacy of our fusion method to mitigate hallucinations of LVLs.

## References

- [1] Jinze Bai, Shuai Bai, Yunfei Chu, Zeyu Cui, Kai Dang, Xiaodong Deng, Yang Fan, Wenbin Ge, Yu Han, Fei Huang, Binyuan Hui, Luo Ji, Mei Li, Junyang Lin, Runji Lin, Dayiheng Liu, Gao Liu, Chengqiang Lu, Keming Lu, Jianxin Ma, Rui Men, Xingzhang Ren, Xuancheng Ren, Chuanqi Tan, Sinan Tan, Jianhong Tu, Peng Wang, Shijie Wang, Wei Wang, Shengguang Wu, Benfeng Xu, Jin Xu, An Yang, Hao Yang, Jian Yang, Shusheng Yang, Yang Yao, Bowen Yu, Hongyi Yuan, Zheng Yuan, Jianwei Zhang, Xingxuan Zhang, Yichang Zhang, Zhenru Zhang, Chang Zhou, Jingren Zhou, Xiaohuan Zhou, and Tianhang Zhu. Qwen technical report. *arXiv preprint arXiv:2309.16609*, 2023. 2
- [2] Jinze Bai, Shuai Bai, Shusheng Yang, Shijie Wang, Sinan Tan, Peng Wang, Junyang Lin, Chang Zhou, and Jingren Zhou. Qwen-vl: A frontier large vision-language model with versatile abilities. *arXiv preprint arXiv:2308.12966*, 2023. 1, 2, 5, 7, 11
- [3] Tim Brooks, Aleksander Holynski, and Alexei A. Efros. Instructpix2pix: Learning to follow image editing instructions. In *IEEE Conference on Computer Vision and Pattern Recognition (CVPR)*, 2023. 4
- [4] Zhaorun Chen, Zhuokai Zhao, Hongyin Luo, Huaxiu Yao, Bo Li, and Jiawei Zhou. Halc: Object hallucination reduction via adaptive focal-contrast decoding. *arXiv preprint arXiv:2403.00425*, 2024. 1, 3
- [5] Wenliang Dai, Junnan Li, Dongxu Li, Anthony Meng Huat Tiong, Junqi Zhao, Weisheng Wang, Boyang Li, Pascale Fung, and Steven Hoi. Instructblip: Towards general-purpose vision-language models with instruction tuning. In *Advances in Neural Information Processing Systems (NeurIPS)*, 2024. 1, 2, 3, 5, 7, 11
- [6] Ailin Deng, Zhirui Chen, and Bryan Hooi. Seeing is believing: Mitigating hallucination in large vision-language models via clip-guided decoding. *arXiv preprint arXiv:2402.15300*, 2024. 3
- [7] Alessandro Favero, Luca Zancato, Matthew Trager, Siddharth Choudhary, Pramuditha Perera, Alessandro Achille, Ashwin Swaminathan, and Stefano Soatto. Multi-modal hallucination control by visual information grounding. In *IEEE Conference on Computer Vision and Pattern Recognition (CVPR)*, 2024. 1, 2, 3, 4, 6, 8, 14
- [8] Chaoyou Fu, Peixian Chen, Yunhang Shen, Yulei Qin, Mengdan Zhang, Xu Lin, Jinrui Yang, Xiawu Zheng, Ke Li, Xing Sun, et al. Mme: A comprehensive evaluation benchmark for multimodal large language models. *arXiv preprint arXiv:2306.13394*, 2023. 1, 2, 4, 5, 8
- [9] Zigang Geng, Binxin Yang, Tiankai Hang, Chen Li, Shuyang Gu, Ting Zhang, Jianmin Bao, Zheng Zhang, Houqiang Li, Han Hu, et al. Instructdiffusion: A generalist modeling interface for vision tasks. In *IEEE Conference on Computer Vision and Pattern Recognition (CVPR)*, 2024. 4
- [10] Anisha Gunjal, Jihan Yin, and Erhan Bas. Detecting and preventing hallucinations in large vision language models. In *AAAI Conference on Artificial Intelligence (AAAI)*, 2024. 1, 2
- [11] Jonathan Ho, Ajay Jain, and Pieter Abbeel. Denoising diffusion probabilistic models. *Advances in neural information processing systems*, 33:6840–6851, 2020. 3
- [12] Qidong Huang, Xiaoyi Dong, Pan Zhang, Bin Wang, Conghui He, Jiaqi Wang, Dahua Lin, Weiming Zhang, and Nenghai Yu. Opera: Alleviating hallucination in multimodal large language models via over-trust penalty and retrospection-allocation. In *IEEE Conference on Computer Vision and Pattern Recognition (CVPR)*, 2024. 3
- [13] Sicong Leng, Hang Zhang, Guanzheng Chen, Xin Li, Shijian Lu, Chunyan Miao, and Lidong Bing. Mitigating object hallucinations in large vision-language models through visual contrastive decoding. In *IEEE Conference on Computer Vision and Pattern Recognition (CVPR)*, 2024. 1, 2, 3, 4, 5, 8, 11, 14
- [14] Xiang Lisa Li, Ari Holtzman, Daniel Fried, Percy Liang, Jason Eisner, Tatsunori Hashimoto, Luke Zettlemoyer, and Mike Lewis. Contrastive decoding: Open-ended text generation as optimization. In *The 61st Annual Meeting Of The Association For Computational Linguistics*, 2023. 1, 3, 11
- [15] Yifan Li, Yifan Du, Kun Zhou, Jinpeng Wang, Wayne Xin Zhao, and Ji-Rong Wen. Evaluating object hallucination in large vision-language models. In *Proceedings of the 2023 Conference on Empirical Methods in Natural Language Processing*, 2023. 1, 2, 4, 5, 7, 11
- [16] Yuanze Lin, Yi-Wen Chen, Yi-Hsuan Tsai, Lu Jiang, and Ming-Hsuan Yang. Text-driven image editing via learnable regions. In *IEEE Conference on Computer Vision and Pattern Recognition (CVPR)*, 2024. 4
- [17] Fuxiao Liu, Kevin Lin, Linjie Li, Jianfeng Wang, Yaser Yacoob, and Lijuan Wang. Mitigating hallucination in large multi-modal models via robust instruction tuning. In *International Conference on Learning Representations (ICLR)*, 2024. 1, 2
- [18] Haotian Liu, Chunyuan Li, Yuheng Li, and Yong Jae Lee. Improved baselines with visual instruction tuning. In *IEEE Conference on Computer Vision and Pattern Recognition (CVPR)*, 2024. 1, 2, 5, 7, 11
- [19] Yassine Ouali, Adrian Bulat, Brais Martinez, and Georgios Tzimiropoulos. Clip-dpo: Vision-language models as a source of preference for fixing hallucinations in lvlms. In *European Conference on Computer Vision (ECCV)*, 2024. 1, 2
- [20] Alec Radford, Jong Wook Kim, Chris Hallacy, Aditya Ramesh, Gabriel Goh, Sandhini Agarwal, Girish Sastry, Amanda Askell, Pamela Mishkin, Jack Clark, et al. Learning transferable visual models from natural language supervision. In *International Conference on Machine Learning (ICML)*, 2021. 2, 3
- [21] Rafael Rafailov, Archit Sharma, Eric Mitchell, Christopher D Manning, Stefano Ermon, and Chelsea Finn. Direct preference optimization: Your language model is secretly a reward model. *Advances in Neural Information Processing Systems (NeurIPS)*, 2024. 2
- [22] Zhiqing Sun, Sheng Shen, Shengcao Cao, Haotian Liu, Chunyuan Li, Yikang Shen, Chuang Gan, Liang-Yan Gui, Yu-Xiong Wang, Yiming Yang, et al. Aligning large multi-

- modal models with factually augmented rlhf. *arXiv preprint arXiv:2309.14525*, 2023. 1, 2
- [23] Hugo Touvron, Thibaut Lavril, Gautier Izacard, Xavier Martinet, Marie-Anne Lachaux, Timothée Lacroix, Baptiste Rozière, Naman Goyal, Eric Hambro, Faisal Azhar, et al. Llama: Open and efficient foundation language models. *arXiv preprint arXiv:2302.13971*, 2023. 2
- [24] Xintong Wang, Jingheng Pan, Liang Ding, and Chris Bie-mann. Mitigating hallucinations in large vision-language models with instruction contrastive decoding. *arXiv preprint arXiv:2403.18715*, 2024. 1, 2, 3
- [25] Spencer Whitehead, Jacob Phillips, and Sean Hendryx. Pre-training multimodal hallucination detectors with corrupted grounding data. *arXiv preprint arXiv:2409.00238*, 2024. 1
- [26] Qinghao Ye, Haiyang Xu, Jiabo Ye, Ming Yan, Anwen Hu, Haowei Liu, Qi Qian, Ji Zhang, and Fei Huang. mplug-owl2: Revolutionizing multi-modal large language model with modality collaboration. In *IEEE Conference on Computer Vision and Pattern Recognition (CVPR)*, pages 13040–13051, 2024. 2
- [27] Shukang Yin, Chaoyou Fu, Sirui Zhao, Tong Xu, Hao Wang, Dianbo Sui, Yunhang Shen, Ke Li, Xing Sun, and Enhong Chen. Woodpecker: Hallucination correction for multimodal large language models. *arXiv preprint arXiv:2310.16045*, 2023. 2
- [28] Zhiyuan Zhao, Bin Wang, Linke Ouyang, Xiaoyi Dong, Ji-aqi Wang, and Conghui He. Beyond hallucinations: Enhancing llms through hallucination-aware direct preference optimization. *arXiv preprint arXiv:2311.16839*, 2023. 1, 2
- [29] Lianmin Zheng, Wei-Lin Chiang, Ying Sheng, Siyuan Zhuang, Zhanghao Wu, Yonghao Zhuang, Zi Lin, Zhuohan Li, Dacheng Li, Eric Xing, et al. Judging llm-as-a-judge with mt-bench and chatbot arena. *Advances in Neural Information Processing Systems (NeurIPS)*, 2023. 2
- [30] Yiyang Zhou, Chenhang Cui, Jaehong Yoon, Linjun Zhang, Zhun Deng, Chelsea Finn, Mohit Bansal, and Huaxiu Yao. Analyzing and mitigating object hallucination in large vision-language models. In *International Conference on Learning Representations (ICLR)*, 2024. 1, 2
- [31] Deyao Zhu, Jun Chen, Xiaoqian Shen, Xiang Li, and Mohamed Elhoseiny. Minigpt-4: Enhancing vision-language understanding with advanced large language models. *arXiv preprint arXiv:2304.10592*, 2023. 2
- [32] Lanyun Zhu, Deyi Ji, Tianrun Chen, Peng Xu, Jieping Ye, and Jun Liu. Ibd: Alleviating hallucinations in large vision-language models via image-biased decoding. *arXiv preprint arXiv:2402.18476*, 2024. 3

# Delve into Visual Contrastive Decoding for Hallucination Mitigation of Large Vision-Language Models

## Supplementary Material

### 7. Details of Visually Contrastive Decoding

#### 7.1. Plausibility Constraints

Based on the contrastive decoding process from (2) in the main paper, it may penalize the entire LVLM’s responses via contrast samples. However, either original or visually changed samples may still generate words related to linguistic standards and common sense. Therefore, inaccurate punishment of these words may cause an unpredictable and even failed response. To tackle this issue, we follow previous works [13, 14] to introduce the plausibility constraint, which avoids the indiscriminate penalization caused by directly applying contrastive decoding to entire responses. The plausibility constraint is triggered by the confidence related to candidate tokens of original visual inputs, which can be formulated as:

$$\begin{aligned} V_{cond}(y_{<t}) &= \{y_t \in V : \\ p_{\theta}(y_t|v, x, y_{<t}) &\geq \beta \max_{\omega} p_{\theta}(\omega|v, x, y_{<t})\}, \\ p_{cd}(y_t|v, v_{cd}, x, y_{<t}) &= 0 \text{ if } y_t \notin V_{cond}(y_{<t}), \end{aligned} \quad (9)$$

where  $V_{cond}$  is the output of LVLMs and  $\beta$  in  $[0, 1]$  is a hyperparameter that controls how aggressive to keep only high-probability tokens (e.g., a higher value indicates a more aggressive manner). Therefore, the probability of other candidate tokens below the constraints is replaced with 0. With the plausibility constraint, contrastive decoding influences the next token predicting behaviors only when the LVLMs are not confident with their prediction. We set  $\beta = 0.2$  by default.

### 8. More Analysis on LVLMs

We provide more analysis of visually changed samples on LVLMs, including more LVLMs (e.g., Qwen-VL [2]), more metrics (e.g., confidence of predictions), and details of POPE benchmarks (e.g., random, popular tasks). In this section, we mainly investigate the behaviors of visually changed samples from the perspective of different LVLMs, in which the conclusions are drawn similarly to the main paper.

#### 8.1. Analysis with Entropy and Confidence

We have discussed the investigation of entropy with InstructBLIP [5] and LLaVA-1.5 [18] in the main paper, which presents the different behaviors of visually changed samples. Here we provide the comparison of entropy with another LVLM, Qwen-VL, as shown in Figure 7. We also

visualize the confidence distribution in Figure 8, where the confidence is estimated from the highest probability of the next-token prediction. The confidence is correlated with the entropy, where the lower confidence induces the higher entropy. We draw several observations:

1) Within the same benchmark (i.e., POPE [15], which focuses on object hallucination and has tasks of three difficulties), the distributions of entropy and confidence are similar across different LVLMs.

2) With similar concepts of changing images (i.e., reducing visual information), the downsample and diffusion noise methods have similar behaviors regarding entropy and confidence on the LLaVA-1.5 and Qwen-VL, while obtaining distinct behaviors on InstructBLIP. The reason could be the different architecture of visual-textual interfaces in LVLMs, where InstructBLIP leverages Q-Former to extract visual features while LLaVA-1.5 and Qwen-VL directly project the image embedding to text embedding via multi-layer perception (MLP) and cross-attention layer, respectively.

Based on the above observations, we argue that the behaviors of visually changed samples vary across LVLMs and benchmarks.

#### 8.2. Analysis with Probability Distribution Distance

We investigate the probability distribution distance (PDD) of visually changed samples across different POPE tasks and LVLMs, which present the similarity of output predictions to original ones, as shown in Figure 9. We find that different visually changed samples have varying PDD distributions across different LVLMs:

1) For InstructBLIP, the influence of each visually changed sample is distinct, where the prediction of image editing and no image methods are centralized at high PDD value, while downsample and diffusion noise methods have the opposite distributions.

2) For LLaVA-1.5, the downsample and diffusion noise methods have similar distributions centralized at lower PDD values, while the image editing method has a distribution with higher PDD values. Different from InstructBLIP, the no image method has a much lower PDD value, which could result from the difference in answering tendency (as shown in Figure 10).

3) However, for the Qwen-VL, the PDD distributions of each visually changed sample are much similar and smoother, meaning that the responses produced by visually changed samples are unpredictable. That is, we cannot determine the impact of downsample or diffusion noise meth-

ods given arbitrary visually changed inputs.

These observations show that LVLMs react with visually changed samples in different ways, which can also have varying impacts on the outcomes of contrastive decoding.

### 8.3. Revision Behaviors

We provide the statistics of revision behaviors and answering tendencies on different benchmarks, as shown in Figure 10 and 11. We find that the answering tendencies of visually changed samples on LVLMs are very different. The InstructBLIP tends to answer “yes” while LLaVA-1.5 is prone to answering “no” for the visually changed samples. Moreover, we also find that no image method obtains valid answers (“yes” or “no”) on LLaVA-1.5 and Qwen-VL, which differs from the behavior on InstructBLIP. This evidence demonstrates the answering tendency varies across different LVLMs, resulting in different behaviors of contrastive decoding with visually changed samples. Such a conclusion can also be obtained from the observation of revision behaviors, which shows that different visually changed samples present different trends in revising answers of different LVLMs (e.g., image editing on POPE-A achieves the least revise-wrong on InstructBLIP but the highest one on Qwen-VL).

### 8.4. Pairwise Overlap of Rectified Answers

We visualize the pairwise overlap of rectified answers of LVLMs in Figure 12, and draw several observations:

1) For InstructBLIP and LLaVA-1.5, all pairs of CDs have low IoUs, demonstrating the rectified samples resulting from visually changed samples are different and non-overlapping. Moreover, the IoU of rectified samples from applying downsample and diffusion noise methods is rather higher than other pairs, indicating a similar type of changes on images could lead to similar outcomes.

2) For Qwen-VL, the results are different from those on the other two LVLMs. On the POPE benchmark, the overlap between downsample and diffusion noise is higher. Meanwhile, on the MME benchmark, the overlaps among downsample, diffusion noise, and no image methods exhibit significantly higher IoUs. On the contrary, the image editing method shows notably low IoUs with the other methods. The evidence suggests that the reduction of visual information may have a similar influence on predictions of Qwen-VL, whereas the editing of contents impacts its predictions differently.

From these observations, we conclude that for the different LVLMs, the behaviors of visually changed samples could vary, encouraging us to develop a fusion method to leverage the strengths of different visually changed samples to mitigate hallucinations.

## 9. More Ablation Studies

To validate our designs for the fusion method of visually changed samples, we conduct several ablation studies, including the combination of fusion, the choice of fusion weights, and the influence of the extent of visual changes.

### 9.1. Combinations of Fusion

We provide results of exhaustive combinations of entropy-weighted fusion methods ranging from involving two to four visually changed samples, as shown in Table 3. In general, combining more visually changed samples obtains better overall performance. With careful selection, the combination of two visually changed samples (e.g., no image (B) + downsampling (C)) can reach a comparable performance with the combination of all samples. However, it could be difficult to accurately select the optimal combinations when deploying on real-world AI agents. In contrast, our fusion method leveraging all the strengths of different visually changed samples serves as a more general and effective solution to mitigate hallucinations of LVLMs.

### 9.2. Ablation of Metric-Weighted Fusions

As mentioned in Sec. 5.2 of the main paper, when the entropy is higher, the LVM is more likely to yield the hallucinated response, which is more suitable for serving as a contrastive sample. Here, we investigate using different probability-level metrics as a weight for the fusion of visually changed samples. To be more general, we reformulate Eq. (8) of the main paper as:

$$p_{cd}(y_t|v, v_{cd}, x, y_{<t}) = \text{softmax}[\text{logit}_\theta(y_t|v, x, y_{<t}) - \sum_{i=1}^k w_i(\text{logit}_\theta(y_t|v, x, y_{<t}) - \text{logit}_\theta(y_t|v_{cd_i}, x, y_{<t}))], \quad (10)$$

where  $w_i$  is the weight of output distribution for a visually changed sample  $v_{cd_i}$ , which can be metrics we have discussed before, including entropy  $e_i$ , confidence  $c_i$ , unconfidence  $u_i = \frac{1}{c_i}$ , and probability distribution distance  $d_i$ .

The results are shown in Table 4. We find that the entropy-weighted fusion reaches the best performance on overall accuracy, verifying our motivation to combine visually changed samples with entropy as weight. In addition, the unconfidence-weighted (denoted as unconf-weighted) fusion also reaches the best performance, which has a higher performance on MME and a lower performance on POPE, demonstrating that different fusion methods have varying preferences for weighting visually changed samples.

### 9.3. Ablation of Extent of Visual Changes

We investigate the influence of the distortion extent of visually changed samples on different benchmarks from the

perspective of performance and entropy. Concretely, the diffusion noise method increases the uncertainty along with the increasing value of noise step  $N$  of the diffusion process. The downsample method reduces more detailed high-frequency information as the downsample ratio  $r$  increases. For the image editing method, the weight of text guidance  $cf_{g_{text}}$  controls how the edited images relate to the editing textual instruction. As the  $cf_{g_{text}}$  gets higher, the editing results are more likely consistent with the editing textual instruction and even changing the image contents with the queried objects or contents without preserving the similarity to the original image.

We provide the ablation studies of downsample, diffusion noise, and image editing methods in Figure 13, 14, and 15 respectively. Intuitively, the more severe the distortion, the higher the entropy of CDs, increasing the likelihood of inducing hallucinations, where the downsample and diffusion noise method follow this trend. In contrast, the image editing method that inserts the query objects or contents into images directly presents an opposite trend, where the entropy increases as the weight of text guidance decreases. The general trend is that visually changed samples with more distortion acquire higher performance.

## 10. Examples of Image Editing

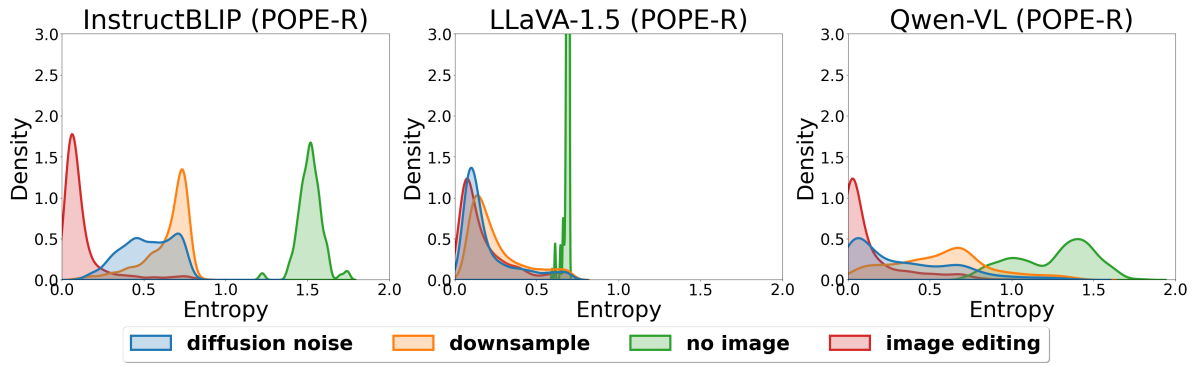
We provide examples of obtaining editing textual instructions from the questions in Table 5. We automatically capture the objects or revise the questions to the affirmative sentences as the editing textual instructions. Figure 16, 17, 18, and 19 are the visual examples of image editing on the POPE and MME benchmarks. The weight of text guidance  $cf_{g_{text}}$  is 20 by default. We find that, when editing images with non-existent objects, the resultant images can either successfully add the queried objects without dramatic distortion or just produce the objects without consistency with the original images. However, when editing images with existent objects, the resultant images may have minor changes in comparison with the original images. This evidence suggests that the image editing method can somewhat reflect the hallucination contents. In addition, when the tasks are more complicated, where the queried contents are the specific landmarks or posters of movies, the image editing still can edit the queried contents into the images if editing models know the contents.

Table 3. The overall results on the Yes-No question tasks, including POPE and MME. The results below are entropy-weighted fusion methods with different combinations of visually changed samples. P-R denotes the *random* task of POPE, P-P denotes the *popular* task of POPE., and P-A denotes the *adversarial* task of POPE. The best performances within each set are marked **bold**, and the second highest performances are underlined.

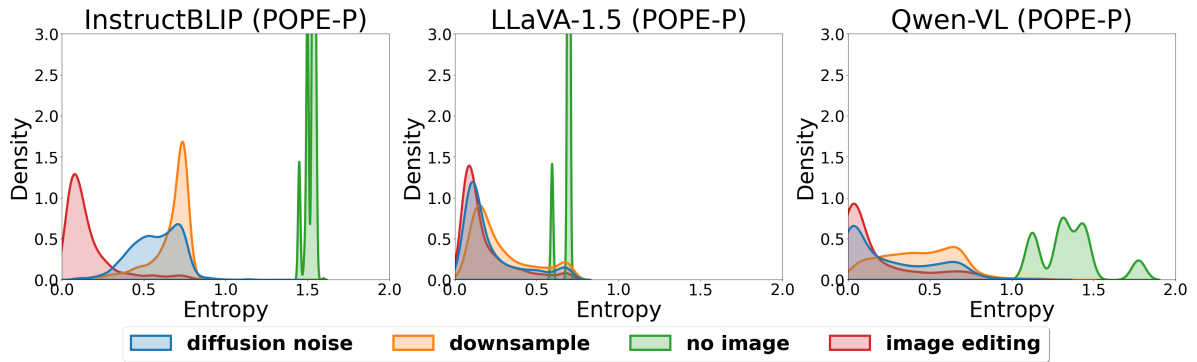
VQA (Y/N)	InstructBLIP				LLaVA-1.5				QwenVL				Overall
Benchmark (Acc)	P-R	P-P	P-A	MME	P-R	P-P	P-A	MME	P-R	P-P	P-A	MME	All
Original	0.825	0.733	0.752	0.688	0.832	0.817	0.788	0.705	0.847	0.851	0.822	0.720	0.785
diffusion noise (VCD [13]) (A)	0.858	0.805	0.779	0.720	0.863	0.842	0.805	0.733	0.865	0.865	0.832	0.747	0.810
no image (M3ID [7]) (B)	0.880	0.835	0.802	0.742	0.871	<u>0.856</u>	<b>0.827</b>	0.732	0.868	0.871	0.837	0.733	0.821
downsample (C)	0.878	0.824	0.801	0.724	<b>0.879</b>	<u>0.856</u>	0.811	<u>0.765</u>	<b>0.875</b>	0.871	0.842	<b>0.764</b>	0.824
image editing (D)	0.860	0.839	<b>0.829</b>	0.747	0.832	0.826	0.811	0.748	0.845	0.838	0.824	<u>0.763</u>	0.814
A+B	0.885	0.847	0.813	0.757	0.872	0.853	0.819	0.747	0.870	0.872	0.841	0.738	0.826
A+C	0.873	0.822	0.797	0.727	0.870	0.855	0.817	0.761	0.872	0.869	0.839	0.739	0.820
A+D	0.865	0.827	0.799	0.743	0.866	0.844	0.818	0.750	0.862	0.862	0.836	0.739	0.818
B+C	0.887	0.850	0.816	0.757	<u>0.877</u>	<b>0.863</b>	0.824	0.758	<b>0.875</b>	<u>0.873</u>	<b>0.844</b>	0.741	0.830
B+D	0.883	0.851	0.815	0.764	0.865	0.849	0.824	0.749	0.869	0.870	0.838	0.744	0.827
C+D	0.874	0.834	0.805	0.740	0.864	0.848	0.817	0.754	0.866	0.867	0.839	0.746	0.821
A+B+C	<b>0.892</b>	0.849	0.818	0.758	0.876	<u>0.856</u>	0.820	0.762	<u>0.874</u>	<b>0.874</b>	<b>0.844</b>	0.742	0.829
A+B+D	0.888	0.852	0.820	0.765	0.865	0.852	<u>0.825</u>	0.754	0.869	0.870	0.840	0.743	0.829
A+C+D	0.878	0.832	0.805	0.740	0.868	0.852	0.820	0.762	0.865	0.870	0.838	0.748	0.823
B+C+D	0.889	<u>0.854</u>	0.822	<u>0.770</u>	0.869	0.854	<u>0.825</u>	<b>0.770</b>	0.873	0.871	<b>0.844</b>	0.748	<u>0.832</u>
A+B+C+D	0.890	<b>0.857</b>	<u>0.828</u>	<b>0.774</b>	0.872	<u>0.856</u>	0.824	0.764	0.872	<u>0.873</u>	<b>0.844</b>	0.749	<b>0.833</b>

Table 4. The overall results on the Yes-No question tasks, including POPE and MME. Please refer to Sec. 9.2 for the formulation of fusion methods. P-R denotes the *random* task of POPE, P-P denotes the *popular* task of POPE., and P-A denotes the *adversarial* task of POPE. The best performances within each set are marked **bold**, and the second highest performances are underlined.

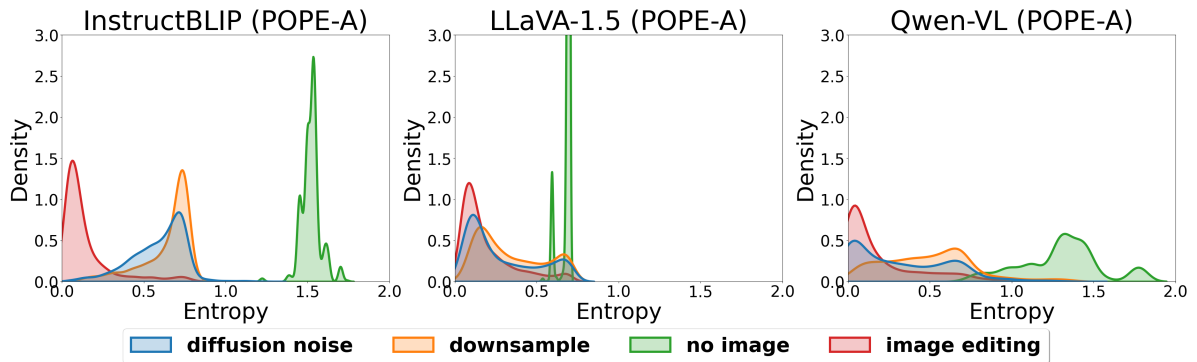
VQA (Y/N)	InstructBLIP				LLaVA-1.5				QwenVL				Overall
Benchmark (Acc)	P-R	P-P	P-A	MME	P-R	P-P	P-A	MME	P-R	P-P	P-A	MME	All
Original	0.825	0.733	0.752	0.688	0.832	0.817	0.788	0.705	0.847	0.851	0.822	0.720	0.785
VCD [13]	0.858	0.805	0.779	0.720	0.863	0.842	0.805	0.733	0.865	0.865	0.832	0.747	0.810
M3ID [7]	<u>0.880</u>	0.835	0.802	0.742	0.871	<b>0.856</b>	0.827	0.732	0.868	<u>0.871</u>	0.837	0.733	0.821
downsample	0.878	0.824	0.801	0.724	<b>0.879</b>	<b>0.856</b>	0.811	0.765	<b>0.875</b>	<u>0.871</u>	0.842	0.764	0.824
IP2P-edit	0.860	0.839	0.829	0.747	0.832	0.826	0.811	0.748	0.845	0.838	0.824	0.763	0.814
naive fusion	0.864	0.840	<b>0.832</b>	<u>0.774</u>	0.862	0.847	<u>0.827</u>	<u>0.779</u>	0.865	0.860	0.839	<b>0.768</b>	<u>0.830</u>
entropy-weighted fusion	<b>0.890</b>	<b>0.857</b>	0.828	<u>0.774</u>	0.871	<b>0.856</b>	0.824	0.764	<u>0.871</u>	<b>0.872</b>	<b>0.844</b>	0.749	<b>0.833</b>
PDD-weighted fusion	0.876	<u>0.849</u>	<u>0.830</u>	0.760	<u>0.872</u>	0.849	0.825	0.755	0.866	0.861	0.838	0.762	0.829
conf-weighted fusion	0.861	0.839	<b>0.832</b>	0.766	0.865	0.845	0.824	0.775	0.862	0.858	0.835	<b>0.768</b>	0.828
unconf-weighted fusion	0.868	0.843	<b>0.832</b>	<b>0.778</b>	0.871	<u>0.853</u>	<b>0.829</b>	<b>0.780</b>	<u>0.871</u>	0.865	<u>0.843</u>	<u>0.767</u>	<b>0.833</b>



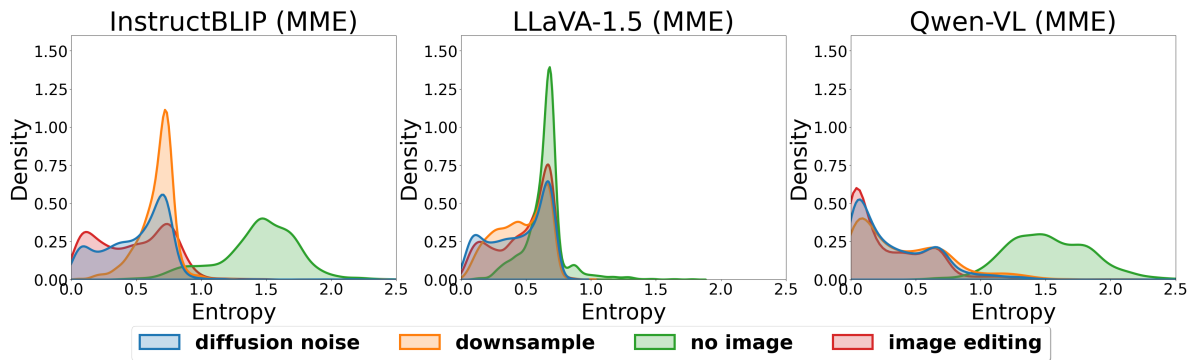
(a) POPE random



(b) POPE popular



(c) POPE adversarial



(d) MME

Figure 7. The analysis of entropy on the POPE and MME benchmarks.

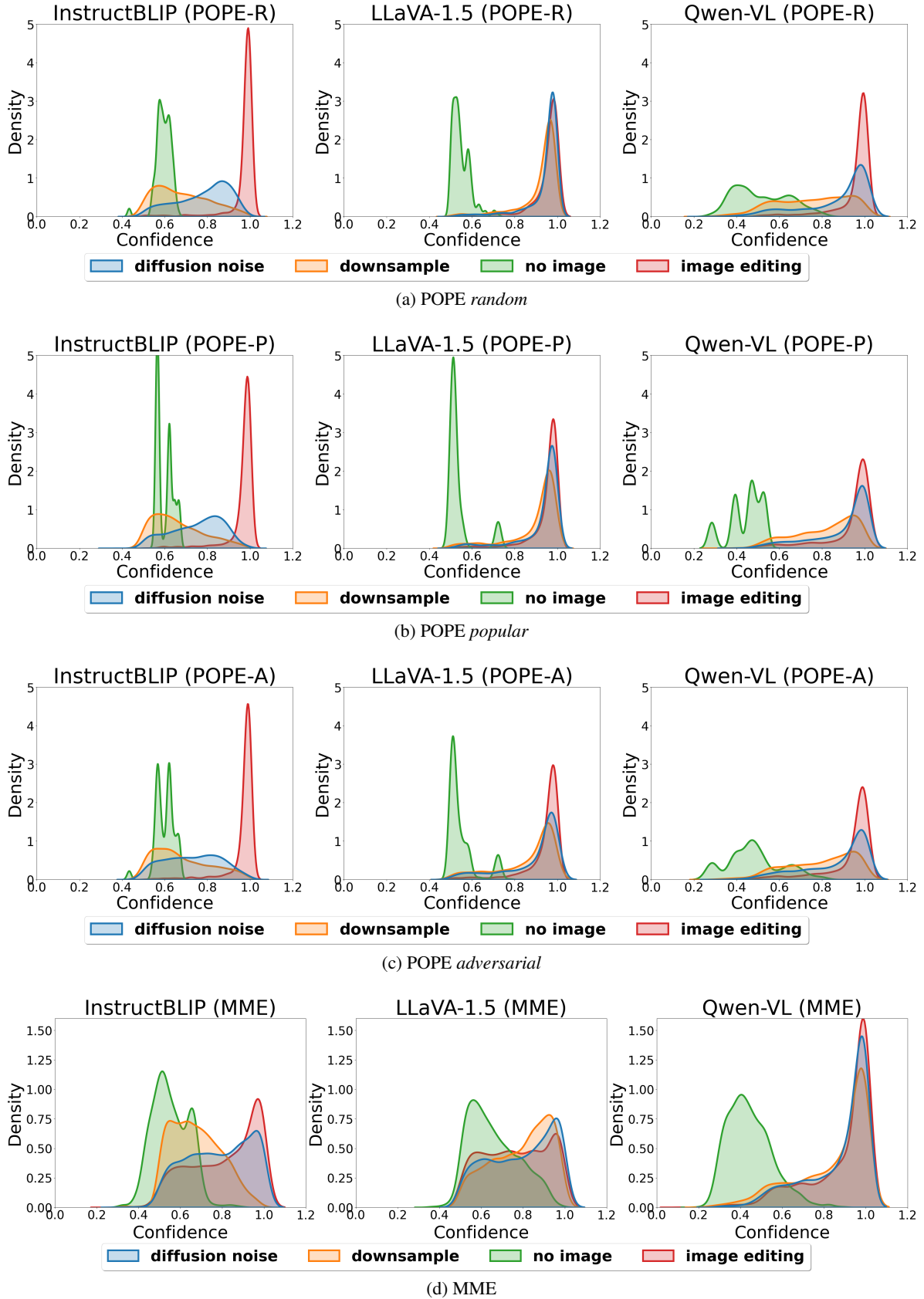
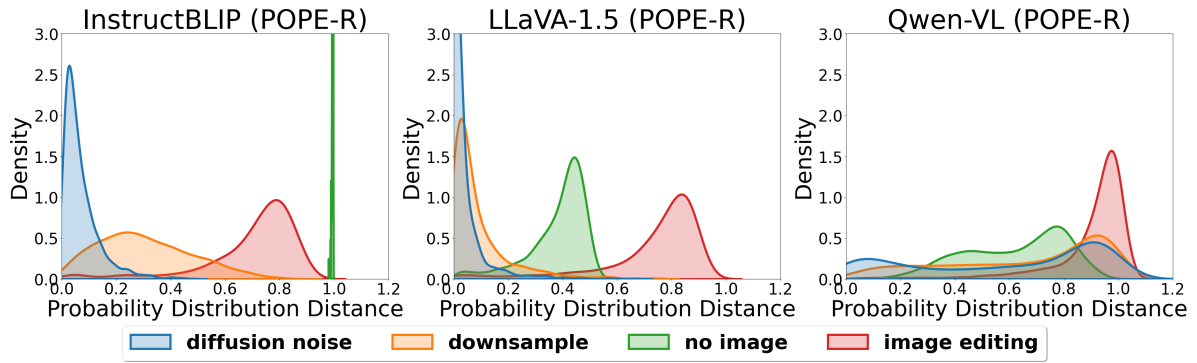
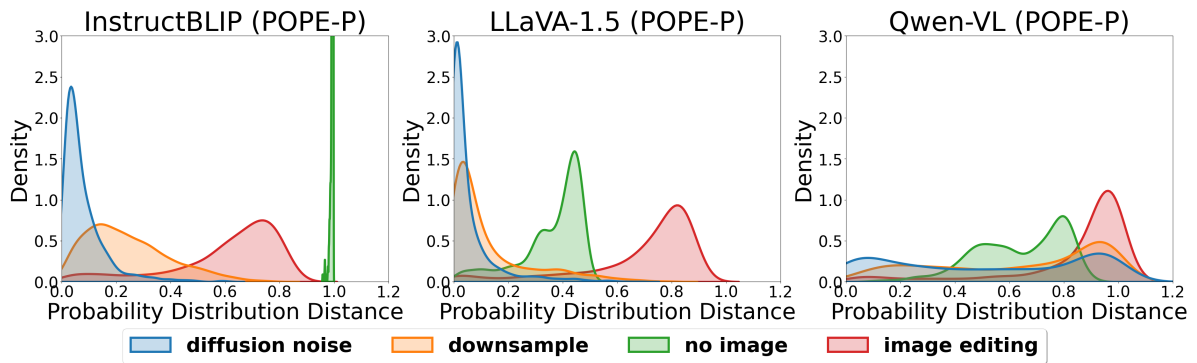


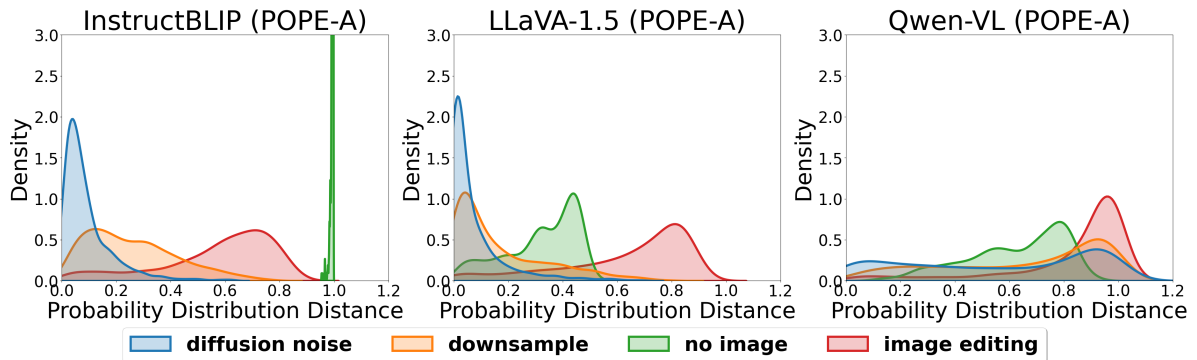
Figure 8. The analysis of confidence on the POPE and MME benchmarks.



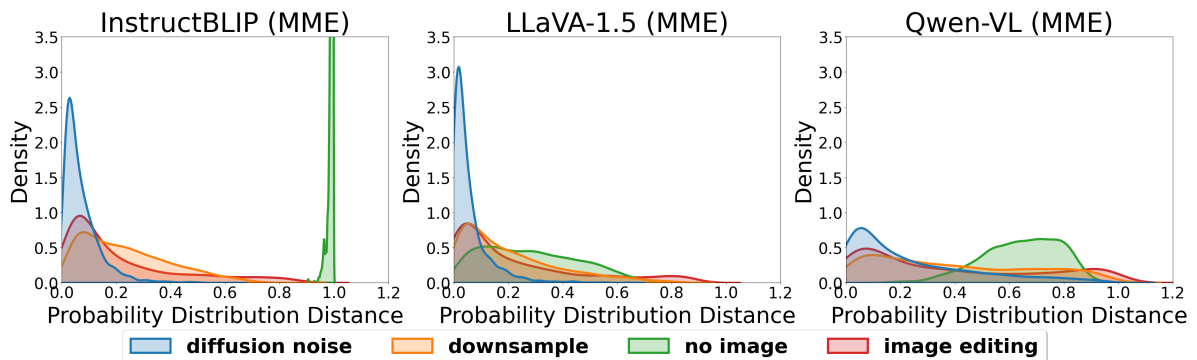
(a) POPE random



(b) POPE popular

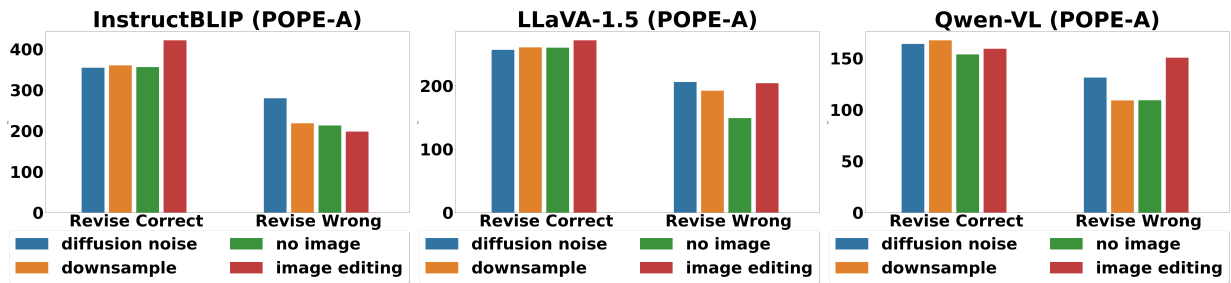


(c) POPE adversarial

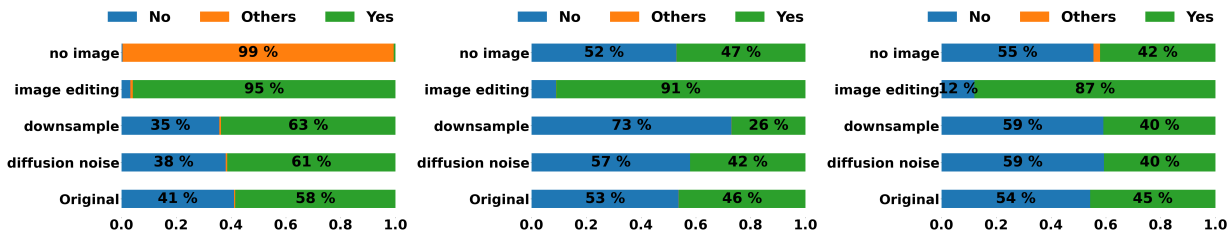


(d) MME

Figure 9. The analysis of probability distribution distance on the POPE and MME benchmarks.

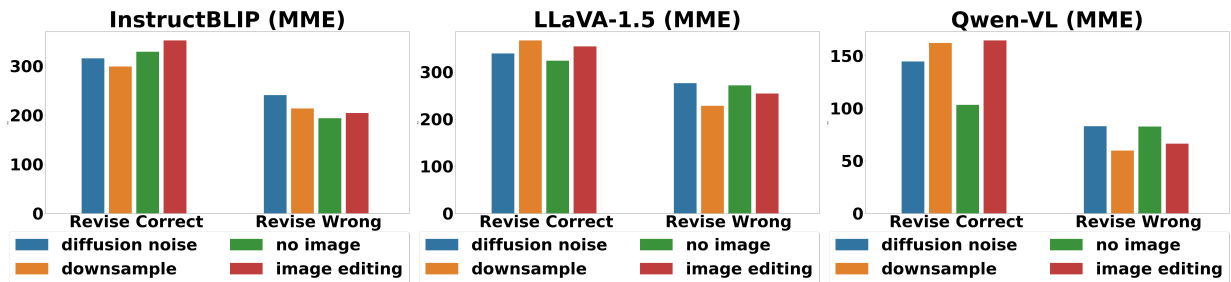


(a) Revision behaviors on POPE

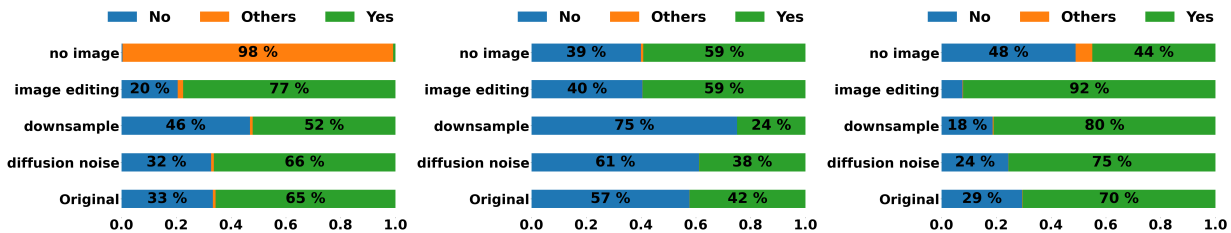


(b) Answering Tendency on POPE

Figure 10. The revision behaviors and answering tendency on POPE benchmark (adversarial task) with different visually changed samples and LVLMs.

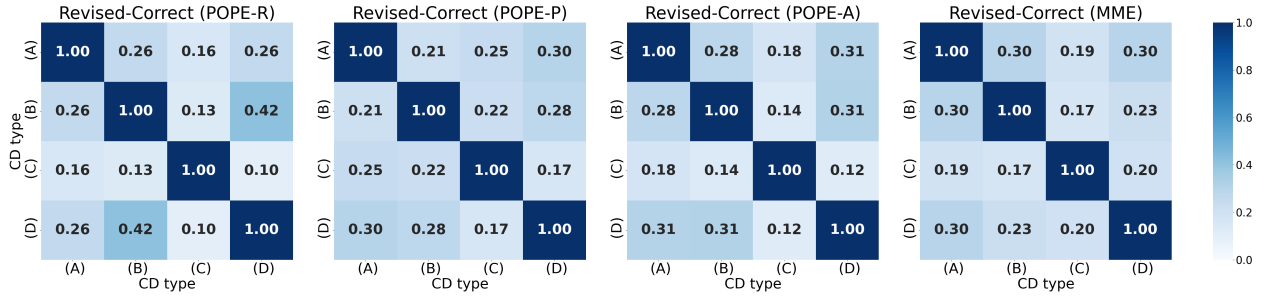


(a) Revision behaviors on MME

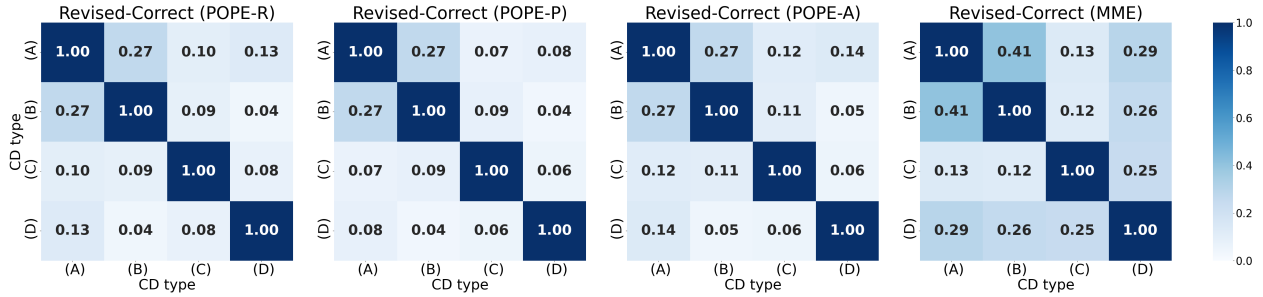


(b) Answering Tendency on MME

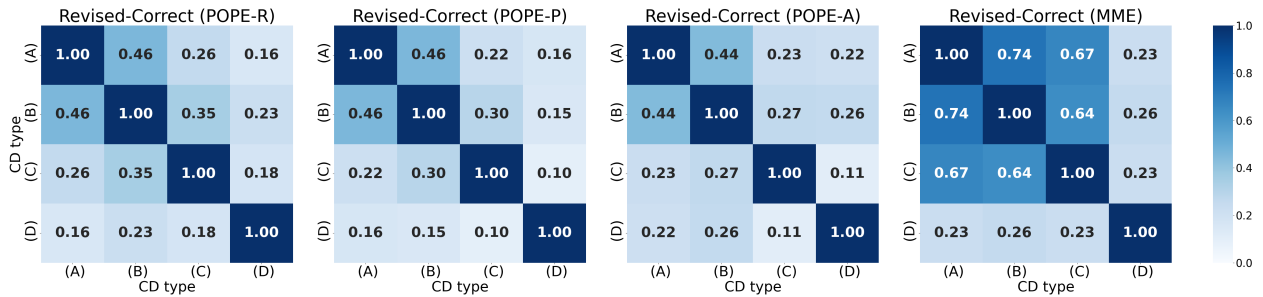
Figure 11. The revision behaviors and answering tendency on MME benchmark with different visually changed samples and LVLMs.



(a) InstructBLIP



(b) LLaVA-1.5



(c) Qwen-VL

Figure 12. The pairwise overlap of revise-correct samples. CD types consist of (A) diffusion noise, (B) downsample, (C) no image, and (D) image editing.

downsample ratio $r$	POPE-R	POPE-P	POPE-A	MME
$r = 32$	<b>0.879</b>	0.817	0.788	0.713
$r = 16$	0.878	<b>0.824</b>	<b>0.801</b>	<b>0.724</b>
$r = 8$	0.866	0.815	0.798	0.720
$r = 4$	0.858	0.812	0.789	0.720

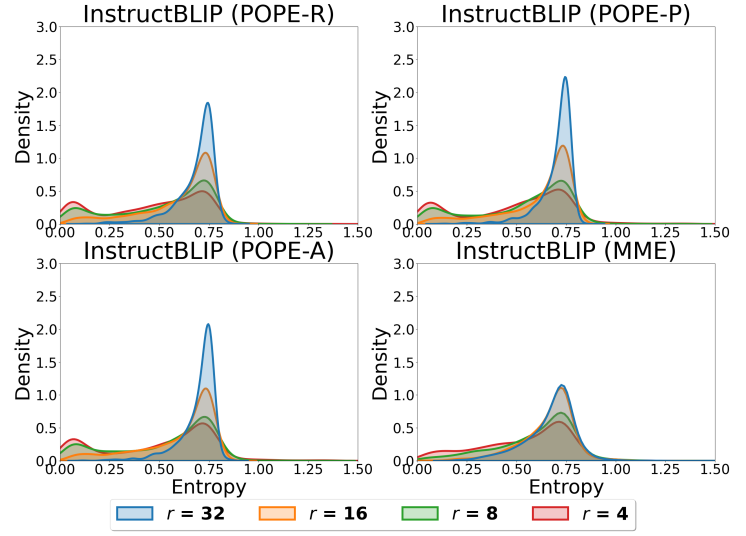


Figure 13. The ablation study of different downsample ratios  $r$  for the downsample method.

noise step $N$	POPE-R	POPE-P	POPE-A	MME
$N = 750$	<b>0.863</b>	<b>0.812</b>	<b>0.795</b>	<b>0.727</b>
$N = 500$	0.858	0.805	0.779	0.720
$N = 250$	0.858	0.805	0.775	0.714
$N = 100$	0.857	0.804	0.771	0.713

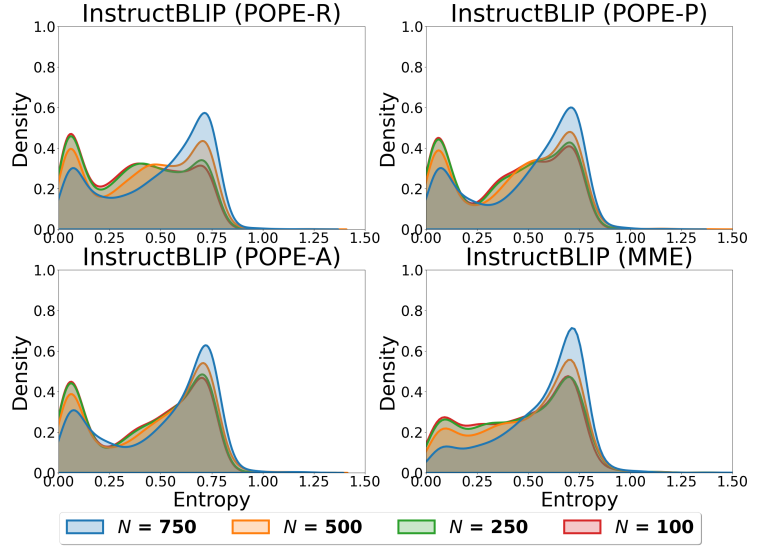


Figure 14. The ablation study of different noise steps  $N$  for the diffusion noise method.

weight of text guidance $cfg_{text}$	POPE-R	POPE-P	POPE-A	MME
$cfg_{text} = 20$	0.860	<b>0.839</b>	<b>0.829</b>	<b>0.747</b>
$cfg_{text} = 15$	0.860	0.837	0.828	0.743
$cfg_{text} = 10$	0.861	0.832	0.814	0.734
$cfg_{text} = 5$	<b>0.868</b>	0.821	0.805	0.714

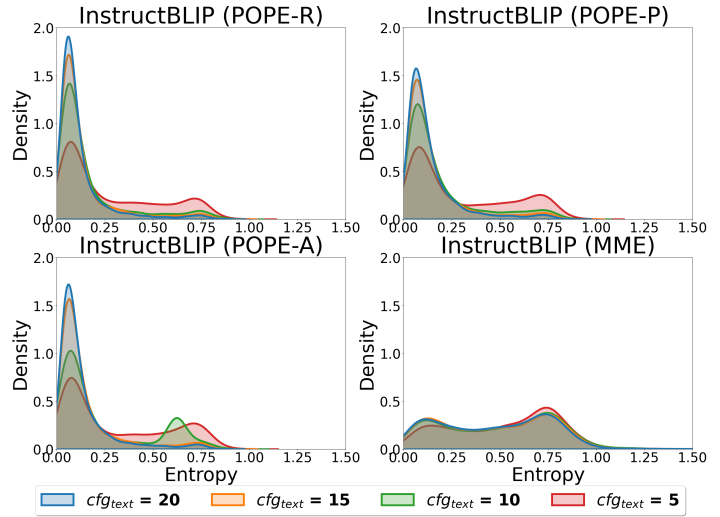


Figure 15. The ablation study of different weight of text guidance  $cfg_{text}$  for the image editing method.

Table 5. The examples of editing textual instruction obtained from the question. For the cognition tasks in MME, we simply duplicate the question for the instruction.

Benchmarks	Tasks	Questions	Editing Textual Instructions
POPE	random, popular, adversarial	Is there a car in the image?	a car
	existence	Is there a elephant in this image?	an elephant
MME	count	Are there a total of two trains in the picture?	a total of two trains
	color	Is there a blue court in the image?	a blue court
	position	Is the vase on the left of the toothbrush?	the vase on the left of the toothbrush
	posters	Is this movie titled a beautiful mind (2001)?	This movie is titled a beautiful mind (2001)
	celebrity	Is the person inside the red bounding box called Sally Field?	the person inside the red bounding box is called Sally Field
	scene	Does this image describe a place of windmill?	a windmill
	landmark	Is this a photo of Clearwater Beach, Florida?	Clearwater Beach, Florida
	artwork	Does this artwork exist in the form of painting?	This artwork exists in the form of painting
	OCR	Is the word in the logo "cold drinks"?	the word in the logo "cold drinks"

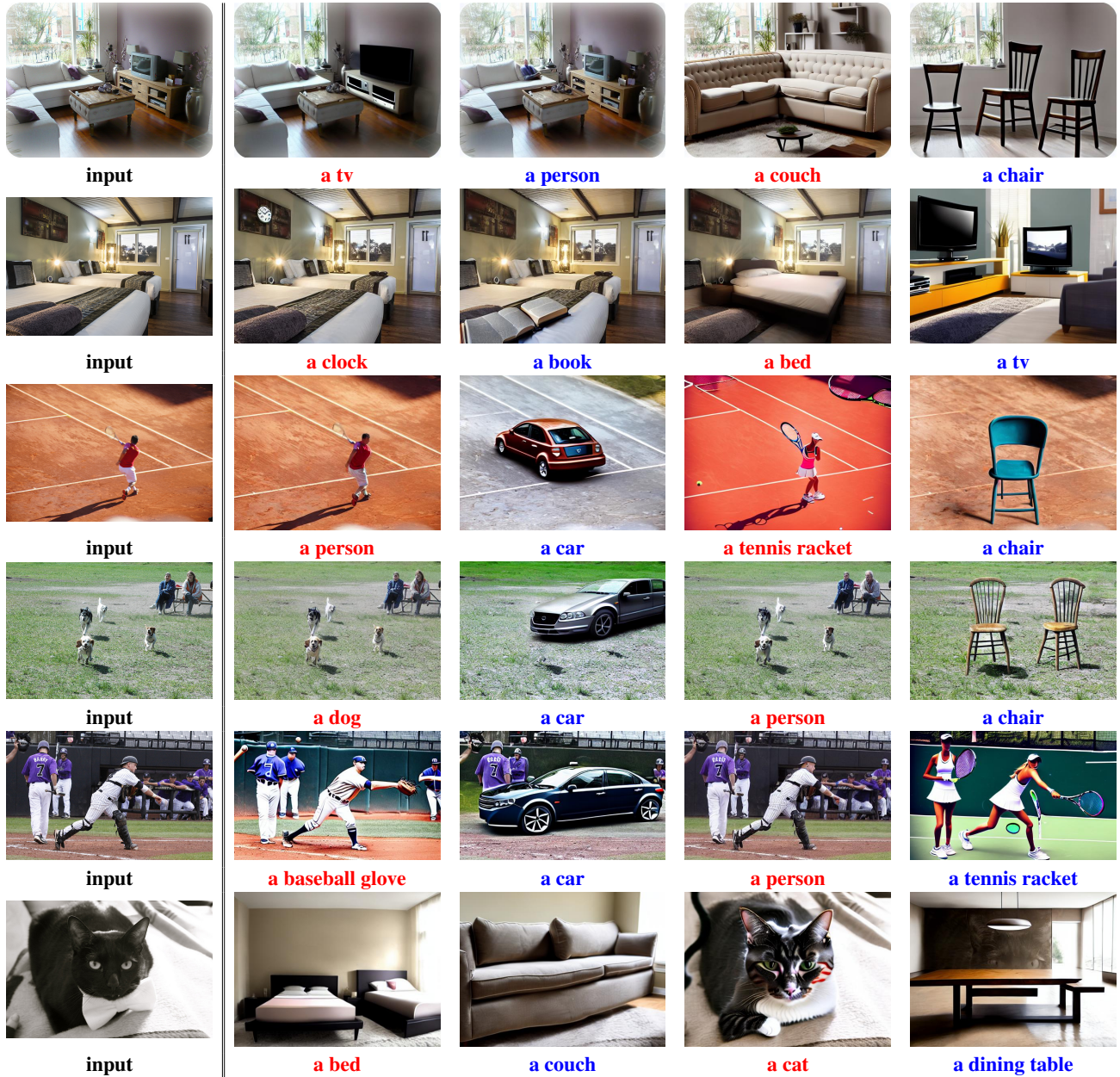
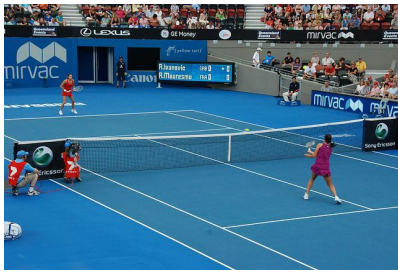


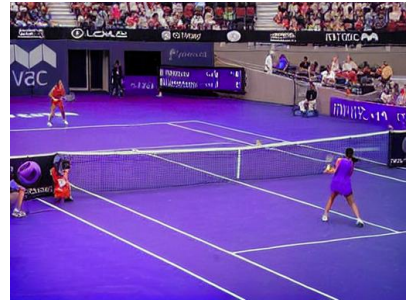
Figure 16. Examples of image editing on POPE benchmark.



**input**



**a blue court**



**a purple court**



**input**



**a white bus**



**a red bus**



**input**



**a train**



**a bed**



**input**



**a person**



**a sink**

Figure 17. Examples of image editing on coarse-grained perception tasks (color and existence) in MME benchmark.



**input**



**a clean room**



**a bookstore**



**input**



**a wind farm**



**a volleyball court outdoor**



**input**



**Ortigia**



**Montmayeur castle**



**input**

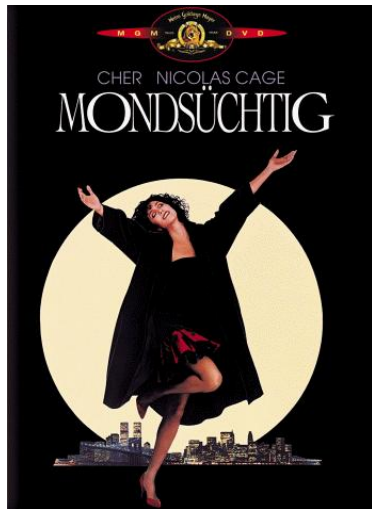


**Grimspound**

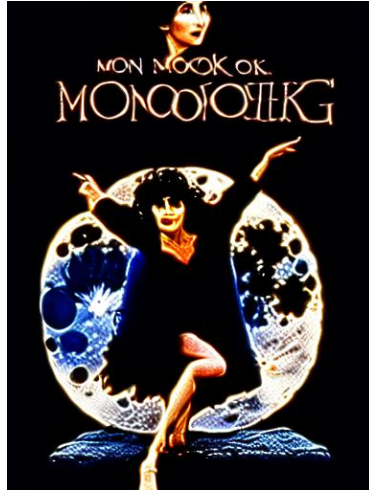


**Lough Owel**

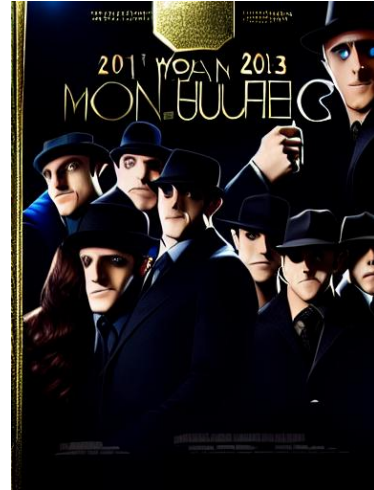
Figure 18. Examples of image editing on fine-grained perception tasks (scene and landmark) in MME benchmark.



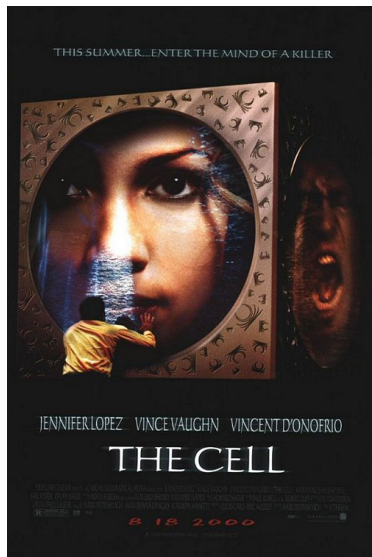
**input**



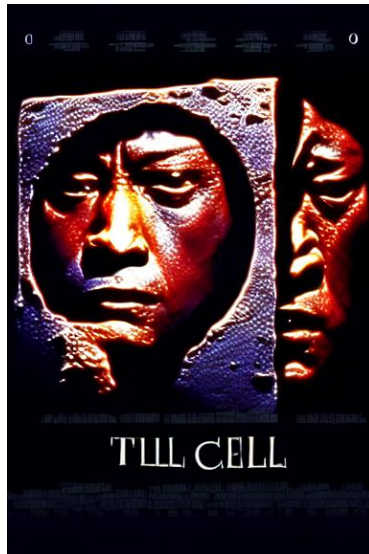
**This movie is titled moonstruck (1987).**



**This movie is titled now you see me (2013).**



**input**



**This movie is titled the cell (2000).**



**This movie is titled the matrix revolutions (2003).**

Figure 19. Examples of image editing on fine-grained perception tasks (posters) in MME benchmark.